

# Machine Vision Inspection of Insect Infested Pistachio Nuts from X-ray Images \*

A. Sim and B. Parvin

Information and Computing Sciences Division  
Lawrence Berkeley Laboratory  
Berkeley, CA 94720

P. Keagy

Western Regional Research Center  
U.S. Dept. of Agriculture  
Albany, CA 94710

## Abstract

An X-ray based system for the inspection of pistachio nuts for internal insect infestation is presented. The novelty of this system is two-fold. First, we construct an invariant representation of infested pistachios from X-ray images that is rich, robust, and compact. This is accomplished by linking the troughs on the image and constructing a joint curvature-proximity distribution table for each nut. Second, we partition the joint distribution table into several regions, where each region is used independently to train a backpropagation (BP) network. The outputs of these subnets are then collectively trained with another BP network. We show that the resulting hierarchical network has the advantage of reduced dimensionality while maintaining a performance similar to the standard BP network.

## 1 Introduction

We present a system that is being evaluated for the inspection of pistachio nuts viewed with an X-ray sensor. The X-ray device reveals internal defects that cannot be otherwise detected by external evidences in the visible domain. In particular, we are interested in identifying insect infested nuts since they contribute to aflatoxin contamination<sup>1</sup> [18]. Presently, only manual inspection based on color, size and density of pistachio nuts is used to remove the externally damaged nuts. A complete automated system should test for internal damages as well, since not all infestations are externally manifested.

In this paper, we outline an inspection system for detecting internal defects which has the following novel features: First, we derive an *invariant* representation that captures pertinent information on infested as well as non-infested nuts; second, we show that by partitioning this invariant representation, a classifier with reduced dimensionality can be constructed. From a geometric perspective, infestation can be characterized by

a dark tunneling appearance in the X-ray image. The tunnel corresponds to the reduced density of the natural content of the nut and to the replacement of that content by a cocoon, insect debris, and air, which have lower X-ray absorption properties. The construction of an invariant representation is complicated by the fact that the tunnel can occur at any spatial location and direction. Some air gaps are due to natural separations between the two halves (cotyledons) of the nut meat. These natural features may be more or less apparent during imaging depending on the resting position of the nut. However, the natural separations are generally accentuated by higher contrast than those that are caused by infestation. In this context, our invariant representation first encodes the tunnels and their magnitude, and then parametrizes this representation with respect to location and orientation. Tunnels can be represented in terms of local positive curvature maxima; these local maxima are then linked to form long curve segments. The invariant and compact representation of these curve segments, with respect to rotation and translation, is then encoded by constructing the distribution of local curvature maxima as a function of distance to the outer boundary of the nut. This distribution is a two dimensional joint histogram with the necessary invariant properties.

The second aspect of our work is in the design of the classifier, which is based on a backpropagation network. We show that partitioning the histogram into several regions, training a network for each region independently, and combining these subnets in a hierarchical fashion can lead to an effective classifier with reduced dimensionality (number of weights) than a standard backpropagation network.

In the next section, a brief summary of the image acquisition system is given. Then in sections 3 and 4, we outline the details of the invariant representation and classification. In each section, we present the intermediate result of our system followed by examples. The paper concludes in section 5 with a summary and a description of future efforts.

\*Research was supported by a grant from the U.S. Dept. of Agriculture, under contract number 6053253132.

<sup>1</sup>Aflatoxin is a natural carcinogenic compound, and its concentration is limited by the U.S. and European regulatory agencies.

## 2 Images

The X-ray images of clean and infested pistachios are captured on photographic film. Nuts from each process stream (Table 2) are individually arrayed on clear adhesive contact paper in one of three orientations (suture plane parallel, perpendicular or at an angle to the film plane) and X-rayed<sup>2</sup>. Films are handled in the dark and exposed without film holders. Twelve bit digital images are obtained from the films at a resolution<sup>3</sup> of  $(0.125\text{mm})^2/\text{pixel}$ . The X-rayed nuts are then opened to determine the presence of insect damage. An image of a clean nut will have the following characteristics: a bright area representing the nut meat, surrounded by a small dark gap between the nut meat and the shell, and a little brighter nut shell outside the kernel. Often there is a dark gap between the two halves of the kernel. The dark areas generally have sharp edges. An insect-infested nut has additional dark areas in the kernel which have been caused by insect bites or tunneling. Figure 1 shows representative images of clean and insect infested pistachios.

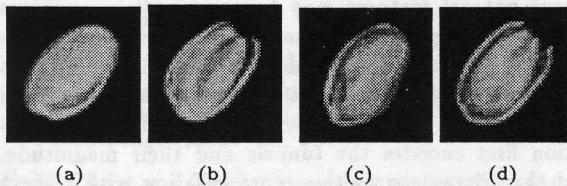


Figure 1: X-ray images of pistachios: (a) & (b) clean and (c) & (d) infested

## 3 Invariant Representation

An ideal representation should capture meaningful features with maximum compactness for effective classification. In this context, the low level representations should be rich, stable, and invariant to the rotation and translation of the object in the image plane as well as in the 3-D space. Compactness in representation can be achieved by encoding the low level features so that similar structures at different spatial locations have the same representation. For example, a cocoon on the left or right side of the nut should be represented identically. In our system, the ideal properties of the low level features are captured by computing the surface curvature at each pixel position. Curvature measurements are invariant to translation and rotation, and their positive local maxima identify the positions of troughs. However, other maxima may also be the results of natural

<sup>2</sup> 90 seconds at 25 keV [0.25 mm Be window] with a Faxitron series X-ray system 4380N, Hewlett Packard, McMinnville, OR; Industrex B film, Eastman Kodak, Rochester, NY

<sup>3</sup> using a Lumiscan 200 film scanner, Lumisys, Sunnyvale, CA

surface properties of the pistachio nut such as the split cotyledon. Still, we assert that curvature maxima on the natural surface have higher magnitude, statistically, at a given distance from the nut boundary when these are compared to those curvature maxima, obtained at the identical distance from the nut boundary, that are due to the infestation. Compactness is achieved by parametrizing curvature features as a function of their distance from the boundary of the nut. This parametrization is constructed as a two dimensional histogram that encodes the curvature-distance joint distribution. We suggest that this histogram corresponds to the signature, or a finger print, that can characterize an infested or clean nut, and we present results to that effect. The system architecture is shown in figure 2, and the details of the above computational steps are outlined below.

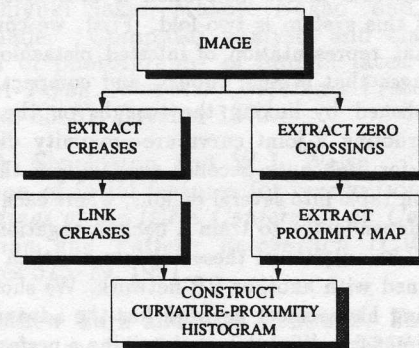


Figure 2: Processing steps

The tunnels are localized by grouping local positive curvature maxima, where curvature corresponds to the differential surface properties of the local intensity distribution for the projected image of the tunnel. Curvature is computed from the first and second fundamental forms. These forms uniquely determine certain local invariant quantities of a 3-D surface, where invariance is expressed in terms of translation, rotation, and scaling for X-ray images. Faux and Pratt [5] expressed the first and second fundamental forms in parametric space. However, from a computational perspective, it is desirable to express these forms in Cartesian space. Let a point on the surface be defined as  $P = x\vec{i} + y\vec{j} + z\vec{k}$ ; then the first and the second fundamental forms are computed to be:

$$G = \begin{bmatrix} 1 + \left(\frac{\partial z}{\partial x}\right)^2 & \frac{\partial z}{\partial x} \frac{\partial z}{\partial y} \\ \frac{\partial z}{\partial x} \frac{\partial z}{\partial y} & 1 + \left(\frac{\partial z}{\partial y}\right)^2 \end{bmatrix} \quad (1)$$

$$D = \frac{1}{n} \begin{bmatrix} \frac{\partial^2 z}{\partial x^2} & \frac{\partial z}{\partial x} \frac{\partial z}{\partial y} \\ \frac{\partial z}{\partial x} \frac{\partial z}{\partial y} & \frac{\partial^2 z}{\partial y^2} \end{bmatrix} \quad (2)$$

The normal curvature of a surface is the curvature of the intersecting curve between the surface and the plane



containing the surface normal and tangent vector to the curve. The directions in which the normal curvature becomes maximum or minimum are called principal directions corresponding to the principal curvatures. The normal curvature is defined as [5]:

$$K_n = \frac{\dot{X}^T D \dot{X}}{\dot{X}^T G \dot{X}} \quad \text{where } \dot{X}^T = \left[ \frac{\partial z}{\partial x} \quad \frac{\partial z}{\partial y} \right] \quad (3)$$

Through elimination and the solution of a pair of simultaneous equations, the following quadratic equation is obtained, where the roots of this equation correspond to maximum and minimum principal curvatures.

$$\begin{aligned} & (g_{11}g_{22} - g_{12}g_{21})k_n^2 \\ & - (g_{11}d_{22} + d_{11}g_{22} - 2g_{12}d_{12})k_n \\ & + (d_{11}d_{22} - d_{12}d_{21}) = 0 \end{aligned} \quad (4)$$

Figure 3 shows the curvature features corresponding to the images shown in figure 1. On these images, white pixels correspond to troughs (positive curvature maxima) and black pixels to ridges (negative curvature maxima) respectively.

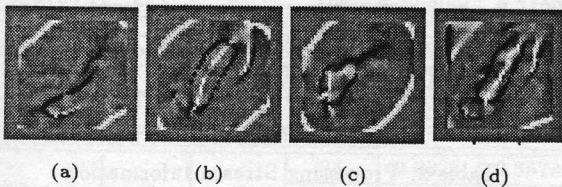


Figure 3: Maximum principal curvatures of surface intensity: (a) & (b) clean and (c) & (d) infested

Once local curvature maxima are determined, they are linked together and long segments are constructed. The steps leading to the extraction of trough segments are enumerated below.

1. Smooth the original image with a Gaussian kernel,
2. Compute the curvatures at each pixel on the smooth image,
3. Threshold the curvature image for troughs,
4. Thin the thresholded image using the non-maximal suppression [3] method. The idea is to keep only the troughs whose maximum curvature is the local maximum, and
5. Link the thinned troughs using a hysteresis [3] method. The hysteresis linking method consists of a high and a low threshold. All points above the high threshold are marked as trough points, and similarly, those points below the low threshold are marked as non-trough points. The points between the low and high thresholds can only be traversed from those troughs that are marked by the high threshold.

The result of linking troughs are shown in figure 4. These images are computed with high threshold of 0.99, low threshold of 0.89, and the kernel size of 1.5 for Gaussian smoothing. These parameters are found to be experimentally appropriate for the nut size, and the expected size of the cocoon that is generated through infestation.

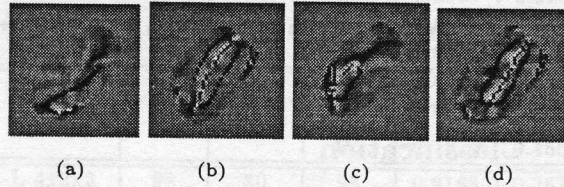


Figure 4: Result of linking for troughs: (a) & (b) clean and (c) & (d) infested

In the next step of the computational process, we compute the distance from each trough point to the boundary of the nut. This is accomplished by first extracting the boundary of the nut with the zero-crossings of the Difference of Gaussian (DoG) filter, and then computing the chamfer image. The chamfer image generates a distance map from edges. The map has a zero value on the edge and increases monotonically from the edge. Figure 5 shows the chamfer images obtained from the boundaries of the nuts shown in figure 1. Once the prox-

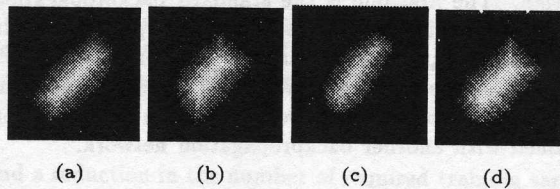


Figure 5: Chamfer images of boundaries of the nut: (a) & (b) clean and (c) & (d) infested

imity map is computed, the two dimensional joint distribution of the curvature-distance table is constructed. Figure 6 shows the cumulative curvature-distance joint histogram for a clean and an infested pistachio, corresponding to the second and the fourth images from example respectively.

In figure 6, the distribution indicates that high curvature activities are more localized, at a given distance from the boundary, for clean pistachios than infested pistachios.

In the next section, we show that the joint distribution has the necessary information content to identify the infested nuts in the population.

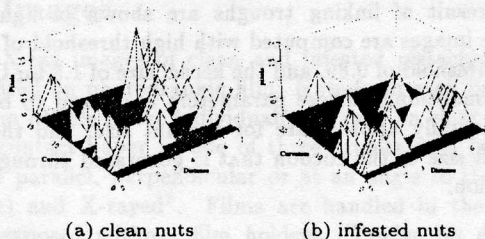


Figure 6: Joint histograms of curvature and proximity values

## 4 Classification

In the design of the classifier, we experimented with several indexing schemes, such as Bidirectional Associative Memory [9] and backpropagation neural network paradigms. The latter consistently produced more favorable results. This is in part due to the large variation in pattern structure and the presence of similar patterns among clean and infested pistachios. The basis for classification is the joint distribution of the curvature-distance table. The curvature values range from 0 to 7.5, and are partitioned into 16 groups, with the distance values ranging from 0 to 9, partitioned into 10 groups. The table is further quantized, as shown in table 1, to reduce the size of the network used for classifying based on the joint distribution and consequently, the size of the training set. The training is based on the backpropagation algorithm. We have experimented with two strategies for further refinement of the classifier design. The first one is the standard backpropagation technique for training a network from a population. In the second approach, we partition the joint distribution table into several regions, where each region is used independently to train a network. These subnets are then trained with another backpropagation network.

Curvatures	Distances		
	1 2 3 4	5 6 7	8 9 10
1 2 3 4	group 1	group 2	group 3
5 6 7 8	group 4	group 5	group 6
9 10 11 12	group 7	group 8	group 9
13 14 15 16	group 10	group 11	group 12

Table 1: Quantization of joint histogram of the curvature and proximity values

The backpropagation (BP) algorithm is a supervised training technique. In the rest of this section, we first evaluate the performance of a standard BP network, then compare its results with the hierarchical one. In the standard implementation of the backpropagation algorithm, we use a three layer network and create a sequential array of the joint distribution table as the input

to this network. The learning rate and the momentum factor are set at 0.1 and 0.9 respectively. These parameters are selected to maintain a balance between achieving fast convergence and arriving at the desirable local minima. The samples are arranged in different trays, and manually identified as clean or defective nuts. Table 2 tabulates the types of defective nuts in these trays. The training set consists of a sample of 80 clean and infested nuts. The clean and infested nuts are randomly selected from trays M and Q respectively.

Product Stream	% of Total Product	Aflatoxin NG/GM	Aflatoxin % of Crop Toxin	Insects per 100 nuts
M	31.06	0	0	0
Q	0.89	89	37	44
A	10.91	1.4	7	2
D	0.13	91	9	9
I	0.53	97	24	13

Tray	Description
M	Good large nuts
Q	Nuts manually removed
A	Nuts with stained shells
D	Lightly stained nuts
I	Small nuts

Table 2: Processing Stream Information

We construct three sets of testing data. The first and second set have 98 and 100 samples from trays M and Q, respectively. The third set has 452 samples from all the trays. All samples are selected randomly without replacement, and none of the testing samples are included in the training set. The classification results for the backpropagation network with various input size and nodes in the hidden layer are shown in Table 3. The poor performance of the third set is due to the presence of other categories of pistachio nuts, as listed in Table 2, that in addition of being infested or clean, they may have other defects as well. In a usual agricultural setting, the inspection of pistachio nuts is a multi-stage process, where at each stage, different types of defects or nut grades are inspected. For example, nuts with external defects such as stained shells, are removed by a different inspection system all together. The third set of data was constructed as an experiment to test if the multi-stage inspection and grading process can be reduced into one single stage. Our result indicate that a two class image-based recognition system is not capable of discriminating the nuts effectively. Other researchers have explored hierarchical networks for machine vision applications [17] as well. However, our implementation does not use shared weights, nor use more than one hidden layer, and it treats the output of



each subnet as a probability measure. Furthermore, the representation used by other researchers is at the pixel level, and no invariant properties of image features are exploited. In our implementation, we divide the joint distribution of histogram into four or six regions (the number of regions is arbitrary). Each region is then used independently to train a BP network. The results of these subnets are then used as input for the next BP network, as shown in figure 7. The classification results for various network sizes are tabulated in table 4.

NODES	WGT	NTRS	NTES	TPF	FPF
24x12x2	312	80	98	0.7959	0.3265
			100	0.9200	0.2200
			452	0.8214	0.4441
24x6x2	168	80	98	0.8776	0.4082
			100	0.9400	0.2400
			452	0.8571	0.4647
20x10x2	220	80	98	0.7347	0.3265
			100	0.8000	0.1800
			452	0.7411	0.3735
20x5x2	110	80	98	0.7959	0.3061
			100	0.8200	0.2400
			452	0.8125	0.4324
16x4x2	72	80	98	0.7755	0.3469
			100	0.9000	0.2800
			452	0.8482	0.4412
12x4x2	56	80	98	0.6327	0.3673
			100	0.7200	0.3000
			452	0.6429	0.4206
6x3x2	24	80	98	0.9388	0.7755
			100	0.9800	0.7000
			452	0.9018	0.7706

NODES: number of nodes in the networks  
WGT: number of computed weights  
NTRS: number of training samples  
NTES: number of testing samples  
TPF: true positive fraction as the percent of infested nuts actually detected  
FPF: false positive fraction as the percent of clean nuts mistakenly identified as infested

Table 3: Performance of standard backpropagation networks with varying number of nodes and hidden layers

The result from our hierarchical network approach shows a similar performance to the standard backpropagation network, while reducing the dimensionality. As an example, the fourth row (20x5x2, 110 weights) from table 3 and the fifth row (L: 4x2x2, H: 8x4x2, 88 weights) from table 4 indicates that the hierarchical BP network with similar performance to the standard BP network has the reduced dimensionality. The  $\chi^2$  test on this example confirms the result as the  $\chi^2$  value 6.3185 with 6 degrees of freedom. The reduced dimensionality of the network has the benefit of improved convergence time

NODES	WGT	NTRS	NTES	TPF	FPF
L 6x4x2 H 12x8x2	304	80	98	0.7143	0.2857
			100	0.8400	0.2600
			452	0.6786	0.3765
L 6x3x2 H 12x4x2	200	80	98	0.8163	0.3673
			100	0.8600	0.2400
			452	0.7589	0.4471
L 6x2x2 H 12x4x2	152	80	98	0.8367	0.3265
			100	0.8600	0.2000
			452	0.6607	0.4706
L 4x3x2 H 8x4x2	112	80	98	0.7959	0.3673
			100	0.7800	0.2600
			452	0.7321	0.4559
L 4x2x2 H 8x4x2	88	80	98	0.8163	0.3673
			100	0.8400	0.2600
			452	0.7054	0.3765
L 4x1x2 H 8x2x2	44	80	98	0.7143	0.2245
			100	0.7000	0.2400
			452	0.5893	0.3029
L 4x1x2 H 8x1x2	34	80	98	0.7143	0.2449
			100	0.7400	0.2600
			452	0.6250	0.3794

NODES: number of nodes in the networks  
WGT: number of computed weights  
NTRS: number of training samples  
NTES: number of testing samples  
L: lower subnetwork  
H: upper network  
TPF: true positive fraction as the percent of infested nuts actually detected  
FPF: false positive fraction as the percent of clean nuts mistakenly identified as infested

Table 4: Performance of hierarchical backpropagation networks with subnet size of 4 and 6 with varying number of nodes and hidden layers

and a reduction in the number of required training samples.

## 5 Conclusion

An inspection system for the classification of infested and clean pistachios is presented. The novelty of our approach lies in the compact and invariant representation of the image features for recognition. The invariance was expressed in terms of curvature-proximity joint distribution function. Furthermore, we showed that by partitioning the input array and hierarchical organization of the BP network, we could reduce the dimensionality in the network significantly, without the loss of accuracy. This result leads us that we need less number of training samples, and that we can reduce the cost of the inspection of pistachios. We believe that this architecture can be used to inspect other varieties of nuts as well, which is the focus of our current effort.

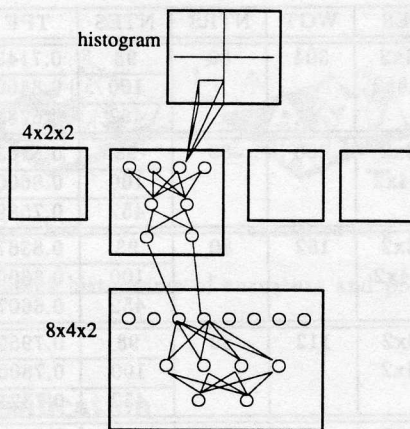


Figure 7: Hierarchical Backpropagation Networks

## References

- [1] R. Anan, K. Mehrotra, C. K. Mohan, and S. Ranka. Analyzing images containing multiple sparse patterns with neural networks. *Pattern Recognition*, 26(11):1717-1724, 1993.
- [2] E. Baum and D. Haussler. What size net gives valid generalization? *Neural Computation*, 1(1):151-160, 1989.
- [3] J. F. Canny. A computational approach to edge detection. *IEEE Transactions on Pattern Analysis and Machine Intelligence*, 8(6):679-698, November 1986.
- [4] L. V. Fausett. *Fundamentals of neural networks : architectures, algorithms, and applications*. Prentice-Hall, Englewood Cliffs, N.J., 1994.
- [5] I. D. Faux and M. J. Pratt. *Computational geometry for design and manufacture*. Ellis Horwood series in mathematics and its applications. Halsted Press, New York, 1979.
- [6] J. M. Gauch and S. M. Pizer. Multiresolution analysis of ridges and valleys in grey-scale images. *IEEE Transactions on Pattern Analysis and Machine Intelligence*, 15(6):635-646, June 1993.
- [7] R. C. Gonzalez and R. E. Woods. *Digital image processing*. Addison-Wesley, Reading, Mass., 1993.
- [8] P. M. Keagy, B. Parvin, and T. F. Schatzki. Machine recognition of naval orange worm damage in x-ray images of pistachio nuts. *Optics in Agriculture, Forestry and Biological Processings*, SPIE 2345, 1994, in press.
- [9] B. Kosko. *Neural networks and fuzzy systems : a dynamical systems approach to machine intelligence*. Prentice Hall, Englewood Cliffs, NJ, 1992.
- [10] A. D. Kulkarni. *Artificial neural networks for image understanding*. Van Nostrand Reinhold, New York, N.Y., 1994.
- [11] S. Y. Kung. *Digital neural networks*. Prentice-Hall information and system sciences series. Prentice-Hall, Englewood Cliffs, N.J., 1993.
- [12] L. Lam, S. Lee, and C. Y. Suen. Thinning methodologies - a comprehensive survey. *IEEE Transactions on Pattern Analysis and Machine Intelligence*, 14(9):869-885, September 1992.
- [13] S. Lu and A. Szeto. Hierarchical artificial neural networks for edge enhancement. *Pattern Recognition*, 26(8):1149-1163, 1993.
- [14] W. K. Pratt. *Digital image processing*. Wiley, New York, N.Y., 1991.
- [15] T. F. Schatzki and P. M. Keagy. Effect of image size and contrast on the recognition of insects in radiograms. *Optics in Agriculture*, pages 182-188, 1991.
- [16] B. W. Silverman. *Density estimation for statistics and data analysis*. Monographs on statistics and applied probability. Chapman and Hall, London, 1986.
- [17] S. A. Solla and Y. le Cun. Constrained neural networks for pattern recognition. In P. Antognetti and V. Milutinovic, editors, *Neural networks : concepts, applications, and implementations*, Prentice Hall advanced reference series, pages 142-161. Prentice Hall, Englewood Cliffs, N.J., 1991.
- [18] N. F. Sommer, J. R. Buchanan, and R. J. Fortlage. Relation of early splitting and tattering of pistachio nuts to aflatoxin in the orchard. *Phytopathology*, 76:692-694, 1986.
- [19] V. Vemuri. Artificial neural networks in control applications. In M. C. Yovits, editor, *Advances in computers*, volume 36, pages 203-254. Academix Press, Inc., Boston, 1993.